

Original Research Article

Design and Modeling of PA-10 Virtual Surgery Robot

Carlos Eduardo Fernández-Riomalo*, Héctor Andrés Guástar-Morillo, Oscar Andrés Vivas-Albán

Cauca University, Popayan, Colombia.

ABSTRACT

This paper introduces the implementation of a virtual laparoscopic surgery simulator assisted by robot. This type of simulator requires three robots: an endoscope robot (Hibou robot in this case) and two surgical robots (Lapbot robot and PA-10 robot in this case). The three robots are operated by the joystick in cholecystectomy and included in the motion deformation algorithm, which modifies the organ to contact the end organ of robot PA-10, so as to make the simulator more realistic. This result provides a basis for laparoscopic surgery simulation using three auxiliary robots, which is an ideal method for training new surgeons.

Keywords: *Laparoscopy; Robot Modeling; Virtual Robot; Surgical Robot; Surgical Simulator*

ARTICLE INFO

Received: Mar 1, 2022
Accepted: Apr 14, 2022
Available online: Apr 22, 2022

*CORRESPONDING AUTHOR

Carlos Eduardo Fernández-Riomalo
carlosfr@unicauca.edu.co;

CITATION

Fernández-Riomalo CE, Guástar-Morillo HA, Vivas-Albán OA. Design and modeling of PA-10 virtual surgery robot. Journal of Autonomous Intelligence 2022; 5(1): 62-71. doi: 10.32629/jai.v5i1.507

COPYRIGHT

Copyright © 2022 by author(s) and Frontier Scientific Publishing. This work is licensed under the Creative Commons Attribution-NonCommercial 4.0 International License (CC BY-NC 4.0).
<https://creativecommons.org/licenses/by-nc/4.0/>

1. Introduction

With the passage of time, the application of robot technology in the field of medicine has greatly increased. The accuracy and accuracy of auxiliary robots provide great advantages in heart, gastrointestinal tract, pediatrics, neurosurgery, especially minimally invasive surgery. The challenges posed by the latter operation to surgeons (fatigue, hand shaking, hand eye reversal effect, loss of touch) make the help of machines desirable.

In minimally invasive surgery, laparoscopy^[1,2] is a relatively new operation, which is performed through a small hole in the abdomen, where the surgeon inserts surgical instruments and cameras (endoscopy). Although this procedure has brought great benefits to patients (lower possibility of infection, less pain and shorter hospitalization), it poses a greater challenge to surgeons because laparotomy is different from small hole surgery.

Among the auxiliary robots for laparoscopic surgery, Da Vinci^[3,4] stands out. It has three surgical arms remotely operated by surgeons and an endoscope arm that transmits the internal image of the patient's abdomen. Other surgical assistants who only operate endoscopy include robot Lapman^[5], robot Ensoassist^[6], and robot Aesop^[7].

As noted above, surgeons face increasing challenges. Therefore, training these new technologies is of great importance. The computer simulator provides a high-fidelity system to provide training for laparoscopic practice. There are several types of coaches. The physical type^[8-10] has a real artificial trunk and a real instrument; Virtual types (such as LapMentor^[11], Mentice^[12], LapSim^[13] and Da Vinci Skills Simulator^[14]) are mainly based on computer simulation and have important realistic features, such as bleeding when cutting fabric or smoke generated by cauterizer.

The Cauca University in Popayan, Colombia, has been working on a virtual surgical simulator for several years^[15], which has two robots: a surgical robot (called Lapbot^[16]) and an endoscope bracket (called Hibou^[17]). The simulator is programmed to perform cholecystectomy, using a joystick device that manipulates a virtual camera (Hibou robot) to position it where intervention is needed, and a robot carrying the necessary surgical instruments (Lapbot robot with instruments: scalpel, clip and cautery).

However, in order to complete the simulator, a second instrument handling robot is required. Since these two robots have actual prototypes made a few years ago, another robot that can work with the current Lapbot is needed. The simplest choice is to copy such a robot, but in order to test and compare its performance with other types of robots, it is decided to implement a commercial robot in the current simulator in order to make its own prototype in the near future. Therefore, Mitsubishi PA10 robot^[18,19] is selected for industrial and medical research.

This article shows a complete surgical simulator, including contact and deformation algorithms,

which increases its authenticity. The main contribution of this article is to complete a robotic surgical simulator, which is the first such simulator in Colombia. It can not only train new surgeons, but also introduce the country to the latest development of surgical robots being developed in the world.

This paper is divided into the following parts: the second part introduces Lapbot and Hibou robots; the third part discusses the design and modeling of PA-10 robot; the fourth part is about software development; the fifth part is the main conclusion of this paper.

2. Lapbot and Hibou robot

The Lapbot robot^[16] has 9 degrees of freedom, 6 active joints and 3 passive joints to ensure that a fixed point is maintained when passing through the trocar (abdominal cavity hole). All joints are rotary, but the first joint is prismatic. **Figure 1** shows the kinematic structure of the Lapbot robot, in which the ring between joints 7 and 8 represents the channel through the abdominal cavity. D_i and R_i refer to the distance according to Dombre and Khalil^[20].

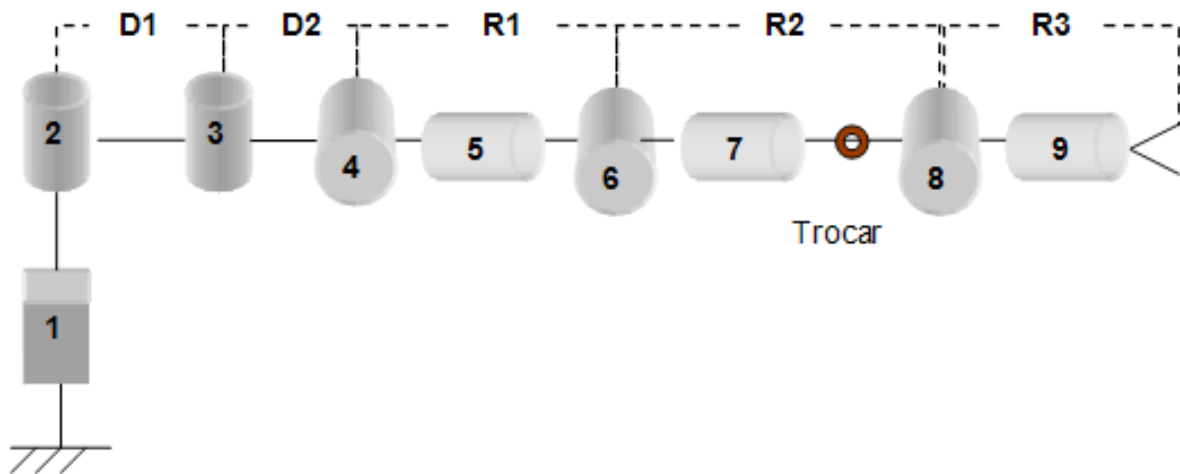


Figure 1. Construction Lapbot robot.

Hibou robot^[17] is designed to support the camera or endoscope of the patient’s abdomen. It consists of seven rotating joints: five active joints and two passive joints, which also ensure the fixed point above the abdominal cavity. **Figure 2** shows the structure of the robot. The trocar is located between joints 5 and 6.

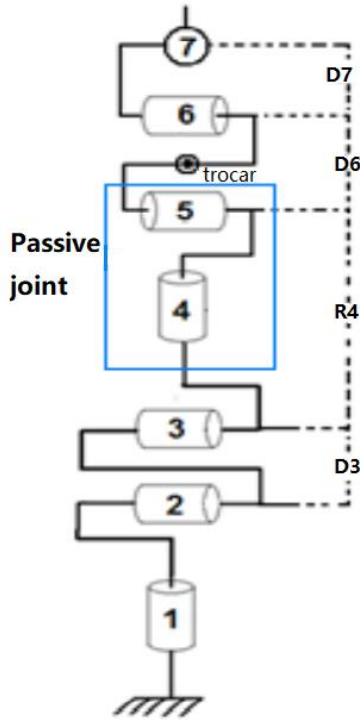


Figure 2. Construction Robot.

As mentioned above, the two robots already have the first real prototype (**Figure 3**).



Figure 3. Lapbot and Hibou robot prototypes.

3. Design and Modeling of PA-10 Robot

3.1 Robot parameters PA-10

PA-10 is a seven degree of freedom robot with seven rotating joints and a parallel wrist shaft. It is

made by Mitsubishi and is very popular in process automation (**Figure 4**).

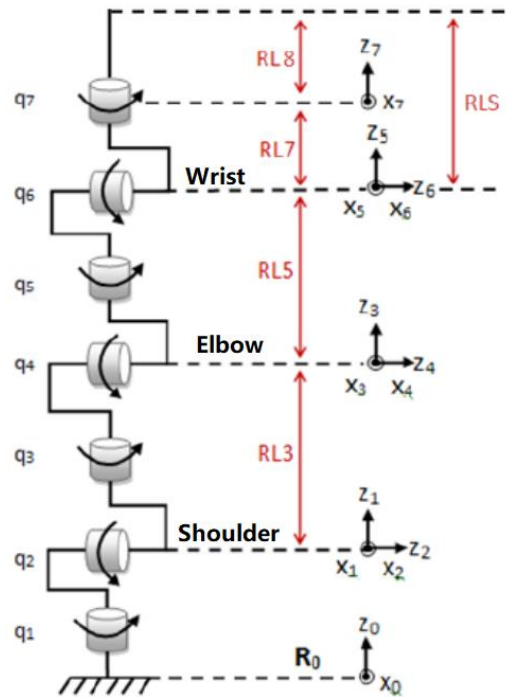


Figure 4. Kinematic structure of PA-10 robot.

According to the analysis of Dombre and Khalil^[20], the corresponding geometric parameter table (**Table 1**) is obtained where j represents the joint number; σ_j refers to the joint type (rotation joint is 0, and prism joint is 1); α_j is the angle between axes z_j ; d_j represents the distance between axes z_j ; θ_j represents the rotation joint variable or angle between shafts x_j ; finally, r_j represents the distance x_j between variable joint prisms or axes.

Table 1. Geometric parameters of PA-10 robot

j	σ_j	α_j	d_j	θ_j	r_j
1	0	0	0	θ_1	0
2	0	-90	0	θ_2	0
3	0	90	0	θ_3	RL3
4	0	-90	0	θ_4	0
5	0	90	0	θ_5	RL5
6	0	-90	0	θ_6	0
7	0	90	0	θ_7	RL7
8	0	0	0	0	RL8

3.2 Design and simulation of PA-10 robot

The design of PA-10 robot is carried out

through the CAD software solid edge, which allows the preliminary design of the moving parts of the robot. Firstly, each part of the robot is designed as an environmental part. Then, use the joint environment, assemble the created parts and observe the interaction between them so as to position the end organ in the desired position (**Figure 5**).

The environment also allows setting the material type of the robot and adding the rotation axis to the design, so as to calculate the inertia parameters such as mass, volume and mass center to determine the inertia moment required by the robot dynamic model (**Table 2** and **Table 3**).



Figure 5. Design of PA-10 robot based on CAD software.

Table 2. Dynamic parameter value (first moment of inertia)

Joint	Moment of inertia X (kg.m)	Moment of inertia Y (kg.m)	Moment of inertia Z (kg.m)
Joint 1	MX1 -0,001304994	MY1 0,092329145	MZ1 6,263547125
Joint 2	MX2 -0,001295329	MY2 -5,057899222	MZ2 1,107399869
Joint 3	MX3 -0,000439824	MY3 0,053981962	MZ3 2,136038315
Joint 4	MX4 -0,000168414	MY4 -1,380103123	MZ4 0,506695466
Joint 5	MX5 -552544e-05	MY5 0,026990969	MZ5 0,278344664
Joint 6	MX6 768857E-05	MY6 -0,017128284	MZ6 0,050611613
Joint 7	MX7 -142258e-07	MY7 0	MZ7 0,000463004

Table 3. Dynamic parameter value (second moment of inertia).

Joint	X. Moment of inertia of Y and Z (kg. m ²)					
Joint 1	lxx	3,958636584	lyy	3,927444666	lzz	0,051621475
	lxy	Type 896572e-06	lxz	-0,000798989	lyz	0,039349258
Joint 2	lxx	3,034902562	lyy	0,14484614	lzz	2,904476538
	lxy	0,000676965	lxz	-0,000114148	lyz	-0,511540072
Joint 3	lxx	0,792444985	lyy	0,773889573	lzz	0,0294865
	lxy	124651E-05	lxz	-0,000182586	lyz	0,01473708
Joint 4	lxx	0,482682499	lyy	0,063293651	lzz	0,427046066
	lxy	828407E-05	lxz	204521E-06	lyz	-0,126755607
Joint 5	lxx	0,04282409	lyy	0,033653767	lzz	0,013760459
	lxy	13935e-05	lxz	599829E-06	lyz	0,00264512
Joint 6	lxx	0,007625747	lyy	0,006506279	lzz	0,002435758
	lxy	-201906e-06	lyy	797667E-06	lyz	-0,001455902
Joint 7	lxx	0,00011655	lyy	0,000116549	lzz	0,00022816
	lxy	0	lyy	34305E-08	lyz	5.6E-12

Before entering the simulation stage, it is necessary to perform the optimization process to make the robot follow the required trajectory while respecting the crossing conditions of trocar^[2]. For this purpose, the position of the trocar (P_{tr}) must be considered, which is located between the wrist (P_m) and the end effector (P_d). Therefore, there must be a collinear condition between these three points, i.e. these points are aligned at each time point. In addition, the position of the elbow (P_c) should also be

considered, which helps to determine the position of the wrist to meet the collinear condition^[21].

The Levenberg Marquart algorithm, a numerical iterative optimization algorithm, is then used to solve the function that provides six joint unknowns ($\theta_1 \dots \theta_6$)^[22]. In order to do this, we input the required positions of x, y and z into the Levenberg Marquart algorithm, from which three elbow positions (P_c) and three wrist positions (P_m) can be obtained, which ensure the intersection of trocar (please note

that the seventh joint has no effect in the step of passing through abdominal hole). For more details on this process, see [21].

Using the established mathematical model, the PA-10 robot is simulated in Matlab-Simulink environment. These parameters include the values of inertial parameters obtained by the CAD Solid Edge®. In addition, the elbow and wrist position data obtained in the above optimization process are also input into the simulation, and these data will become a part of the inverse geometric model of PA-10 robot. The computed torque control (computed torque

control-CTC)^[20,23] is realized, which allows the on-line equipment to work and obtain the torque of the robot motor, so as to purchase the motor for the further manufacturing of the robot in the future. In order to track various slogans in two-dimensional and three-dimensional range, we conducted a repeated debugging process. **Figure 6** shows the CTC control diagram implemented in the simulation, and **Figure 7** shows the Cartesian error of robot PA-10 in circular motion on XY plane with radius of 0.02 m. The maximum error obtained is 1 mm, indicating that the behavior of the controller is acceptable.

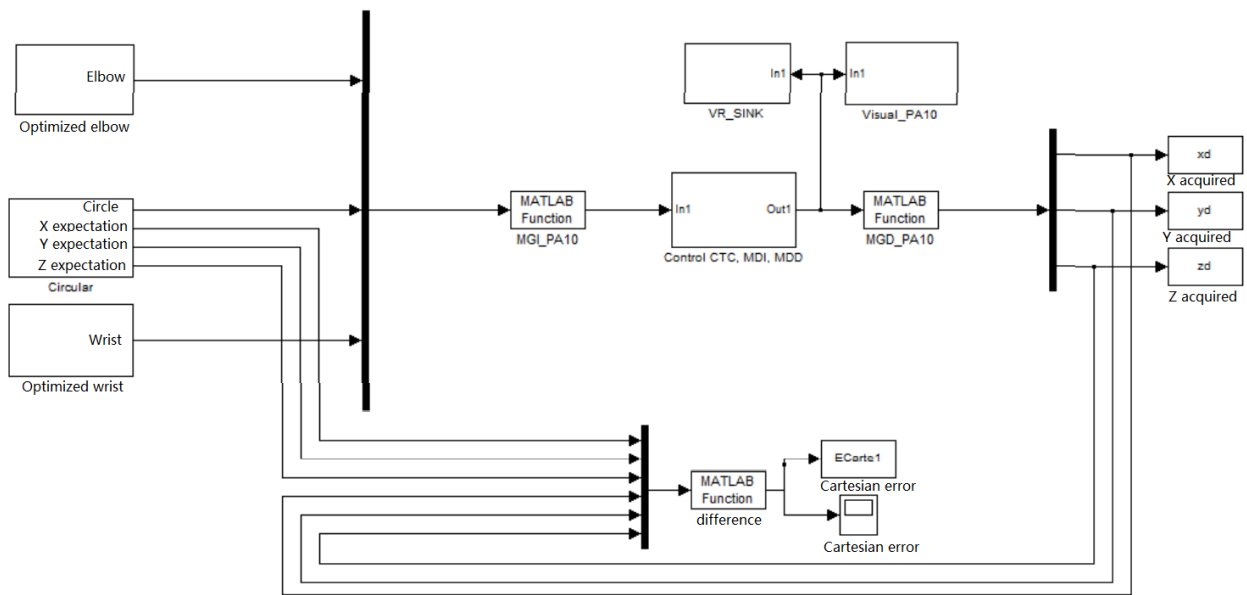


Figure 6. Calculated torque control of PA-10 robot.

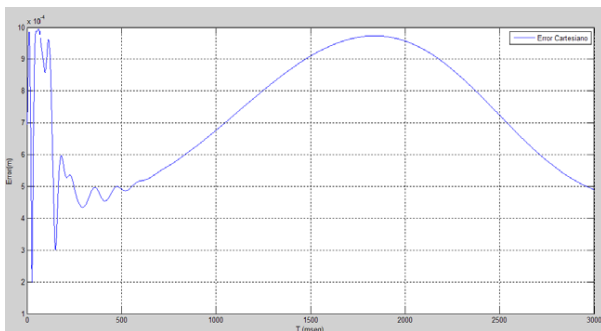


Figure 7. Cartesian error of circular coordinates on XY plane.

4. Virtual simulation software

Using the VTK graphics engine in Visual Studio 2010, the VSRS application program of virtual surgical robot simulator is constructed. The simula-

tor consists of two surgical robots (a Lapbot and a PA-10) and an endoscope robot (Hibou) moved by a joystick (**Figure 8**).

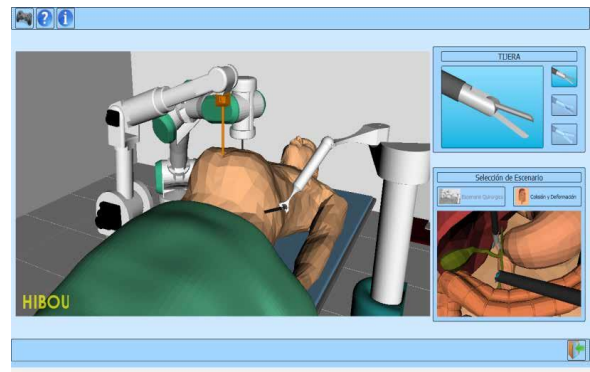


Figure 8. Graphical interface software.

The following two figures (**Figure 9** and **Fig-**

Figure 10 show the use case diagrams of two scenarios (surgery scenario and collision and deformation scenario) for application startup and operation.

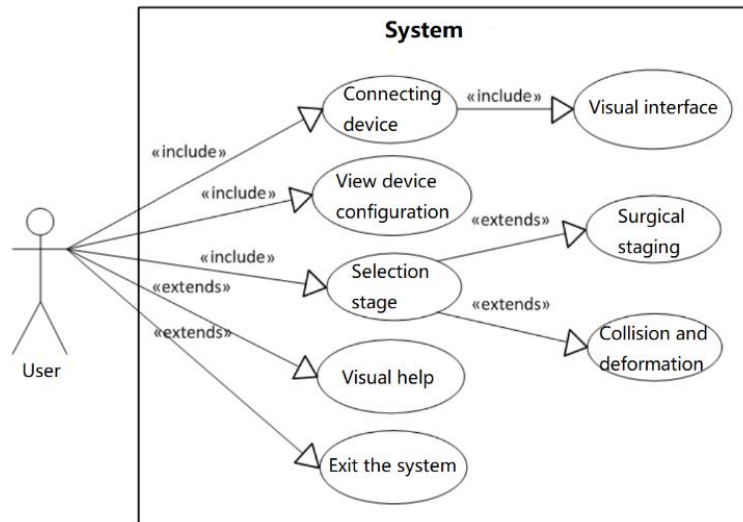


Figure 9. Use case diagram when initializing an application.

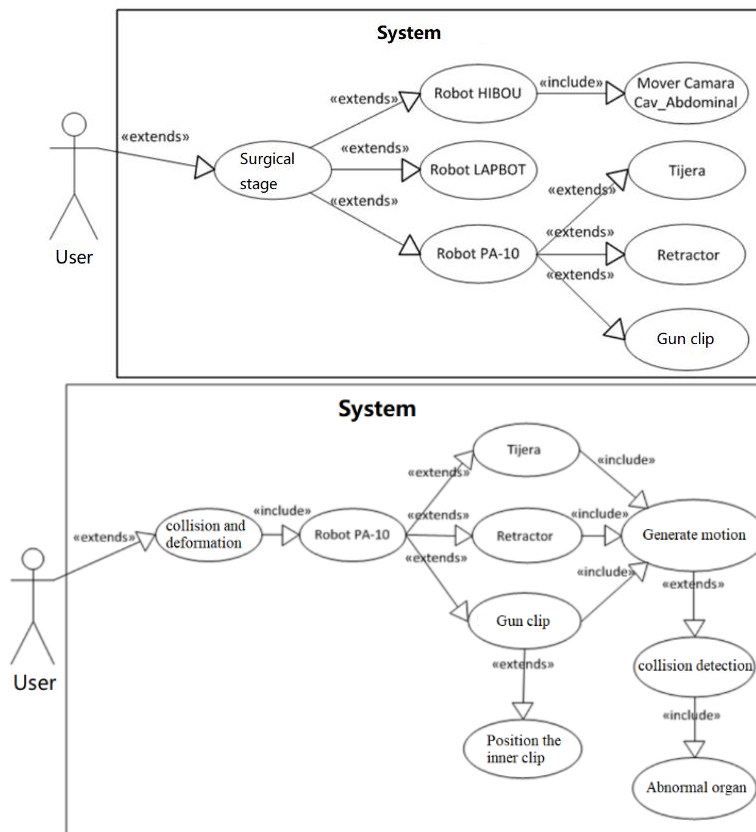


Figure 10. Use case diagram of surgery scenario and collision deformation scenario.

4.1 Software operation

There are two situations for VSRS applications, as described above. In the first (“surgical scene”), there are three windows: the first window shows the environment where the patient contacts the robot; the second is three surgical tools (scissors, retractor

and internal clamping gun) used by PA-10 robot. The third is to observe the interior of the patient’s abdominal cavity through the camera operated by Hibou robot. By selecting the second scenario (“collision and deformation”), the application will deploy the environment shown in the Figure 11.

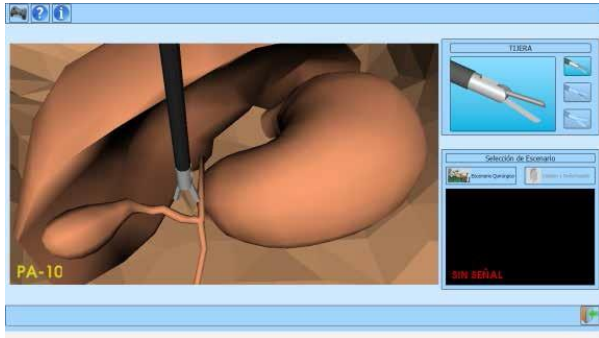


Figure 11. Graphical user interface VSRS (scene collision and deformation).

In the “collision and deformation” scenario, the user can interact with the abdominal organ, causing the end effector of PA-10 to collide with the organ and deform under continuous pressure. See [24] for more details on the deformation algorithm used.

4.2 Collision and deformation

In order to make the end effector of PA-10 robot interact with abdominal organs, the algorithm proposed in document [24] is used. This article explains how to verify the contact between the terminal organ and organ of PA-10.

In order to know the position of the robot terminal organ in the “Robot PA 10” class, a method is defined, which returns the “Matrix” instance of the “vtkMatrix4x4” class. The matrix continuously stores the position of the end organ of the robot, which is calculated by the direct geometric model of the robot.

Before storing the position value of the end effector in the array, scaling is required to couple the

motion of the end effector to the Cartesian position of the mechanism to be deformed. To do this, you must take into account the position of the object in the blender environment (the tool for creating organs), because these positions affect the organs and participants at the time of collision. Therefore, the following procedure needs to be performed.

First, calculate the working area passing through the terminal mechanism by observing all the movements of the fixture from the control device. This can be seen in the **Figure 12**. The workspace displays the distance along the X, Y and Z axes, and its origin is $X = 0.32\text{m}$, $Y = 0.48\text{m}$ and $Z = 0\text{m}$.

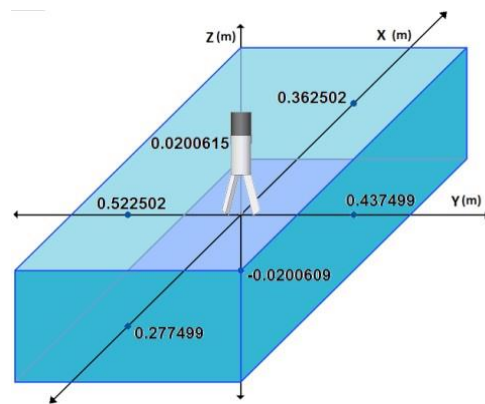


Figure 12. Terminal organ work area.

Calculate the working area of the end effector according to the Cartesian position provided by the mixer, and move the fixture in the mixer environment to the position visually reached by the end effector in the VSRS environment (**Figure 13**). The origin of Cartesian plane in the mixer is $X_b = 0\text{ m}$, $Y_b = 0\text{ m}$, $Z_b = 0\text{ m}$.

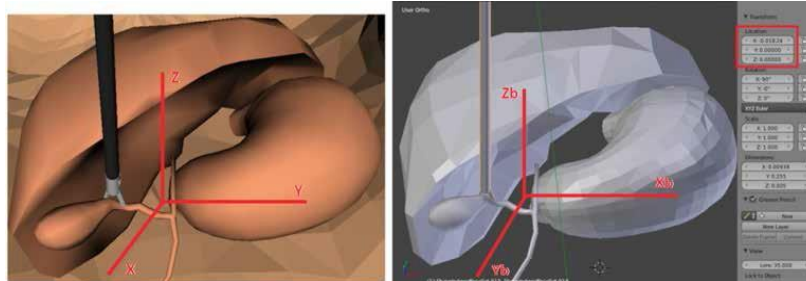


Figure 13. The offset in VSRS generates an offset in the mixer.

In **Figure 14** compare the Cartesian planes of the two environments; At this point, it can be seen that the y-axis offset of VSRS performs offset on the X_b axis of the mixer. Similarly, the X-axis offset of VSRS generates offset on the Y_b axis of the mixer. It

is worth noting that the Y-axis of VSRS is opposite to the X_b axis of the mixer, that is, when y reaches Y_{max} in VSRS, the mixer X_b reaches $X_{b\text{min}}$. A transformation matrix is used to perform this process from the Cartesian plane of VSRS to the Cartesian

plane of blender. The results are also scaled so that the displacement in the mixer corresponds to the appropriate axis in the VSRS application.

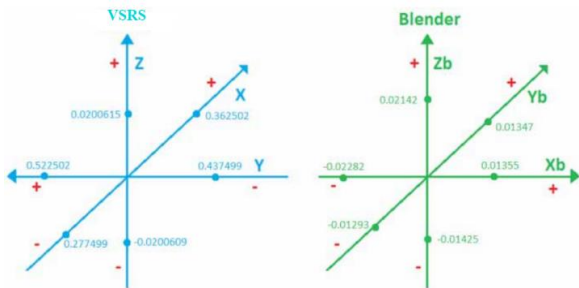


Figure 14. Cartesian plane in VSRS and blender.

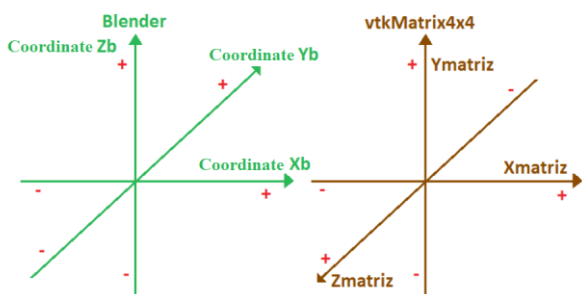


Figure 15. Cartesian plane analysis of blender and VTK matrix4.

After finding the equation to convert the VSRS plane displacement into blender plane, it is necessary to consider the “Matrix” instance plane of “vtkMatrix4x4” (Figure 15).

5. Results

The operation test of PA-10 robot is carried out on VSRS operating table. In order to operate the robot, the control device (joystick or game board) must be connected, and its movement will be carried out by the end effector of the robot according to the instructions. The following (Figure 16) displays the movement of the end organ of the robot. In this case, on the X-axis, it can be observed that due to the movement of the trocar, when the joystick moves to the right, the end organ moves in this direction, but the robot will move in the opposite direction and vice versa (“fulcrum” effect or reverse motion).

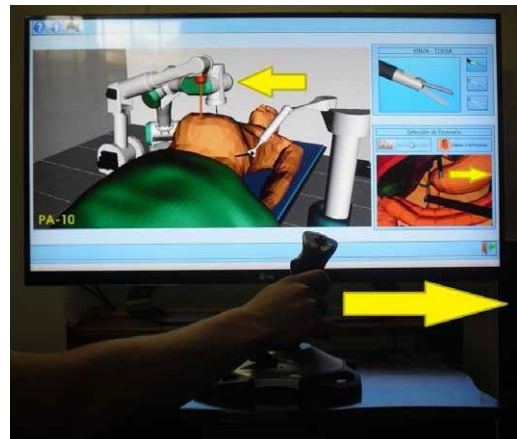


Figure 16. Joystick device and right mobile terminal device.

Figure 17 gives an example of a deformation when the end organ of robot PA-10 is loaded with “scissors” that contacts the volume of the stomach. Figure 18 shows another part of the program. When the robot PA-10 is loaded with the “gun clip” tool, it places its respective internal clamps in the gallbladder tube to interrupt the connection between the liver and the gallbladder for subsequent removal of the gallbladder.

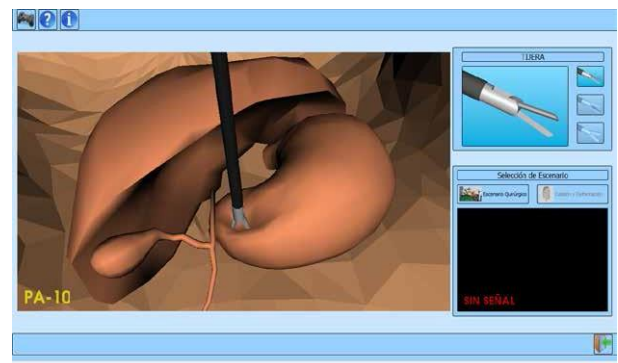


Figure 17. A robot stomach Deformer.

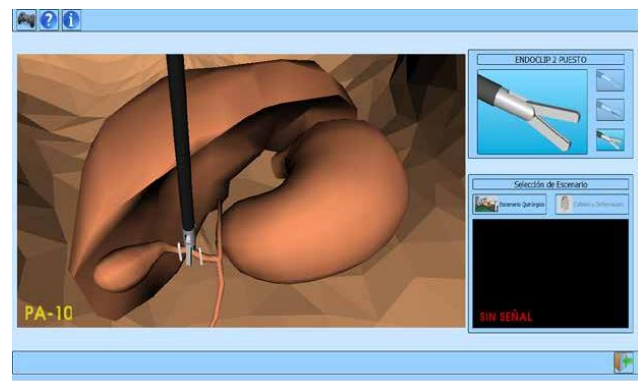


Figure 18. Placement of stent in cystic duct.

Finally, Figure 19 shows the spread of exercise

in the stomach. If the end effector of PA-10 assumes a triangle (dark gray) hitting the propagation center and begins to press inward, the motion propagation must first affect the surrounding triangle, i.e. the black triangle. These triangles constitute the first level of communication. If the pressure continues to be applied on the dark gray triangle, the light gray triangle will also be affected, which is part of the second layer propagation. The same behavior still appears on the X-class triangle. This propagation method allows you to obtain the propagation level of vertices. It is worth noting that this behavior applies to all triangular polygons that make up the object.

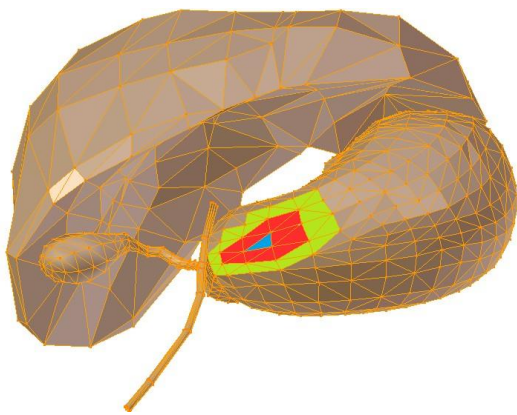


Figure 19. Propagation of motion in triangular meshes.

6. Conclusion

The virtual environment created is called VSRS, which allows users to train in laparoscopic cholecystectomy, because Hibou robot allows to move virtual endoscopy or camera to locate the surgical area, and two surgical robots move the instruments required for such surgery (pliers, scalpel and cautery).

VSRS software reproduces the five stages of cholecystectomy by colliding the instrument carried by one of the two surgical robots with these organs, so as to provide collision and deformation of stomach, liver or gallbladder.

The future work will realize different types of laparoscopic surgery and improve the fidelity of virtual simulation.

Conflict of interest

The authors declare that they have no conflict

of interest.

References

1. Mishra K, Wexner S, Green R. Textbook of practical laparoscopic surgery. New Delhi: Jaypee Brothers Medical Publishers; 2013.
2. Escobar PF, Falcone T (editors). Atlas of single-port, laparoscopic, and robotic surgery: A practical approach in gynecology. New York: Springer; 2014.
3. Ballantyne GH, Moll F. The Da Vinci telerobotic surgical system: the virtual operative field and telepresence surgery. *Surgical Clinics of North America* 2003; 83(6): 1293–1304. doi: 10.1016/S0039-6109(03)00164-6.
4. Smith RD, Truong M. Simulation in Robotic Surgery: A comparative review of simulators of the Da Vinci surgical robot. Oviedo, FLA: Modelbenders Press; 2013.
5. Polet R, Donnez J. Using a laparoscope manipulator (Lapman) in laparoscopic gynecological surgery. *Surgical Technology International* 2008; 17: 187–191.
6. Kommu SS, Rimington P, Anderson C, *et al.* Initial experience with the EndoAssist camera-holding robot in laparoscopic urological surgery. *Journal of Robotic Surgery* 2007; 1(2): 133–137. doi: 10.1007/s11701-007-0010-5.
7. Kraft B, Jäger C, Kraft K, *et al.* The Aesop robot system in laparoscopic surgery: Increased risk or advantage for surgeon and patient? *Surgical Endoscopy* 2004; 18(8): 1216–1223. doi: 10.1007/s00464-003-9200-z.
8. Justo J, Pedroza A, Prado E, *et al.* Un nuevo simulador de laparoscopia [A new laparoscopic simulator] *Medigraphic Artemisa* 2007; 75(1): 19–23.
9. García J, Arias M, Valencia E. Diseño de prototipo de simulador para entrenamiento en cirugía laparoscópica [Prototype design of laparoscopic surgery training simulator]. *Revista Ingeniería Biomédica* 2011; 5(9): 13–19.
10. Sanz S, Sanchez F, Díaz I, *et al.* Validación preliminar del simulador físico Simulap® y de su sistema de evaluación para cirugía laparoscópica [Preliminary validation of simulated physical simulators® and its laparoscopic surgery evaluation system]. *Cirugía Española* 2011; 90(1): 38–44. doi:

- /10.1016/j.ciresp.2011.07.013.
11. Matsuda D, Ono Y, Baba S, *et al.* Positive correlation between motion analysis data on the Lapmentor virtual reality laparoscopic surgical simulator and the results from video tape assessment of real laparoscopic surgeries. *The Journal of Urology* 2008; 179(4): 661. doi: 10.1016/S0022-5347(08)61930-8.
 12. A. Rolls, C. Riga, C. Bicknell, *et al.* A pilot study of video-motion analysis in endovascular surgery: Development of real-time discriminatory skill metrics. *European Journal of Vascular and Endovascular Surgery* 2013; 45(5): 509–515. doi: 10.1016/j.ejvs.2013.02.004.
 13. Patel S, Radia C, Bains S, *et al.* Wii Trauma Centre VS. LapSim: Are modern game consoles comparable to simulators for the development of laparoscopic skills? *International Journal of Surgery* 2013; 11(8): 598. doi: 10.1016/j.ijssu.2013.06.062.
 14. Brinkman W, Luursema J, Kengen B, *et al.* Da Vinci skills simulator for assessing learning curve and criterion-based training of robotic basic skills. *Urology* 2013; 81(3): 562–566. doi: 10.1016/j.urology.2012.10.020.
 15. Guzman Villamarín DE, Vivas Albán OA. Software tool for the practice on robotic surgery. *Ingeniería y Universidad* 2015; 19(1): 7–25. doi: 10.11144/Javeriana.iyu19-1.sprq.
 16. Salinas SA, Vivas Albán OA. Modeling, simulation and control of surgical laparoscopic robot ‘Lapbot’. *Ingeniare. Revista chilena de ingeniería* 2009; 17(3): 317–328. December. 2009. doi: 10.4067/S0718-33052009000300005.
 17. Torres V, Méndez C, Vivas A, *et al.* Diseño y simulación en 3D de un robot porta endoscopio para operaciones de laparoscopia. *The Fifth International Symposium on Electronic Engineering*; Colombia; 2011 Sep; Bucaramanga. 2011.
 18. Kennedy CW, Desai JP. Modeling and control of the Mitsubishi PA10 robot arm harmonic drive system. *IEEE ASME Transactions on Mechatronics* 2005; 10(3): 263–274. doi: org/10.1109/TMECH.2005.848290.
 19. Bompos N, Artemiadis P, Oikonomopoulos A, *et al.* Modeling, full identification and control of the mitsubishi PA-10 robot arm. *IEEE/ASME International Conference on Advanced Intelligent Mechatronics*; 2007 Sep; Zurich (Switzerland). 2007. p. 1–6.
 20. Dombre E, Khalil W. *Modeling, Performance Analysis and Control of Robot Manipulators*. London: Willie; 2010.
 21. Garcés BE, Mora OG, Vivas OA. Study of industrial robots as assistants in laparoscopic surgeries. *Revista Facultad de Ingeniería Universidad de Antioquia* 2009; (47): 91–102.
 22. Levenberg KQ. A method for the solution of certain nonlinear problems in least squares. *Quarterly of Applied Mathematics* 1944; 2: 164–168.
 23. Vivas A. *Diseño y Control de Robots Industriales: Teoría y Práctica [Design and control of industrial robots: Theory and practice]*. Buenos Aires: Elaeph; 2010.
 24. Gómez R, Montero F. *Visualización y deformación de objetos virtuales 3D [visualization and deformation of 3D virtual objects]*. Popayan: Cauca University; 2012.